Hypomorphic caspase activation and recruitment domain 11 *(CARD11)* mutations associated with diverse immunologic phenotypes with or without atopic disease

Check for updates

Batsukh Dorjbal, PhD,[a] Jeffrey R. Stinson, PhD,[a] Chi A. Ma, PhD,[b] Michael A. Weinreich, MD,[b] Bahar Miraghazadeh, PhD,[c,d] Julia M. Hartberger,[e] Stefanie Frey-Jakobs, PhD,[e] Stephan Weidinger, MD,[f] Lena Moebus, MSc,[f] Andre Franke, PhD,[g] Alejandro A. Schäffer, PhD,[h] Alla Bulashevska, PhD,[e] Sebastian Fuchs, PhD,[e] Stephan Ehl, MD, PhD,[e] Sandhya Limaye, PhD,[i] Peter D. Arkwright, FRCPCH, DPhil,[j] Tracy A. Briggs, MBChB, PhD,[j] Claire Langley, PhD,[j] Claire Bethune, MRCP, MRCPath,[k] Andrew F. Whyte, MBBS,[k] Hana Alachkar, MD,[l] Sergey Nejentsev, MD, PhD,[m] Thomas DiMaggio, RN,[b] Celeste G. Nelson, CRNP,[b] Kelly D. Stone, MD,[b] Martha Nason, PhD,[n] Erica H. Brittain, PhD,[n] Andrew J. Oler, PhD,[o] Daniel P. Veltri, PhD,[o] T. Ronan Leahy, PhD,[p] Niall Conlon, FRCPath, PhD,[q] Maria C. Poli, MD,[r] Arturo Borzutzky, MD,[s] Jeffrey I. Cohen, MD,[t] Joie Davis, APRN, APRG,[u] Michele P. Lambert, MD,[v] Neil Romberg, MD,[v] Kathleen E. Sullivan, MD, PhD,[v] Kenneth Paris, MD, PhD,[w] Alexandra F. Freeman, MD,[u] Laura Lucas, RN,[x] Shanmuganathan Chandrakasan, MD,[x] Sinisa Savic, MRCP, FRCPath,[y] Sophie Hambleton, MD, PhD,[z] Smita Y. Patel, MD, PhD, FRCPath,[aa] Michael B. Jordan, MD,[bb] Amy Theos, MD,[cc] Jeffrey Lebensburger, MD,[dd] T. Prescott Atkinson, MD,[ee] Troy R. Torgerson, MD, PhD,[ff] Ivan K. Chinn, MD,[r] Joshua D. Milner, MD,[b]* Bodo Grimbacher, MD,[e]* Matthew C. Cook, MBBS, PhD,[c,d]* and Andrew L. Snow, PhD[a]*
Bethesda, Md; Canberra and Concord, Australia; Freiburg and Kiel, Germany; Manchester, Plymouth, Cambridge, Leeds, Newcastle upon Tyne, and Oxford, United Kingdom; Dublin, Ireland; Houston, Tex; Santiago, Chile; Philadelphia, Pa; New Orleans, La; Atlanta, Ga; Cincinnati, Ohio; Birmingham, Ala; and Seattle, Wash

From [a]the Department of Pharmacology & Molecular Therapeutics, Uniformed Services University of the Health Sciences, Bethesda; [b]the Laboratory of Allergic Diseases, [n]the Biostatistics Research Branch, [o]the Bioinformatics and Computational Sciences Branch, Office of Cyber Infrastructure and Computational Biology, [t]the Laboratory of Infectious Diseases, and [u]the Laboratory of Clinical Immunology and Microbiology, National Institute of Allergy and Infectious Diseases, National Institutes of Health, Bethesda; [c]the Department of Immunology, Canberra Hospital; [d]the Centre for Personalised Immunology, John Curtin School of Medical Research, Australian National University, Canberra; [e]the Center for Chronic Immunodeficiency (CCI), Medical Center–University of Freiburg, Faculty of Medicine, University of Freiburg; [f]the Department of Dermatology, Venereology and Allergology, University Hospital Schleswig-Holstein, Campus Kiel; [g]the Institute of Clinical Molecular Biology, Christian-Albrechts-University of Kiel; [h]the National Center for Biotechnology Information, National Institutes of Health, Department of Health and Human Services, Bethesda; [i]Repatriation and General Hospital, Concord; [j]Paediatric Allergy and Immunology & the Manchester Center for Genomic Medicine, University of Manchester; [k]the Department of Clinical Immunology, Plymouth Hospitals NHS Trust, Plymouth; [l]Immunology, Salford Royal Foundation Trust, Manchester; [m]the Department of Medicine, University of Cambridge; [p]the Department of Paediatric Immunology and ID, Our Lady's Children's Hospital, Crumlin, Dublin; [q]the Department of Immunology, St James's Hospital, Dublin; [r]the Department of Pediatrics, Baylor College of Medicine, and the Section of Immunology, Allergy, and Rheumatology, Texas Children's Hospital, Houston; [s]the Department of Pediatrics, School of Medicine, Pontificia Universidad Catolica de Chile, Santiago; [v]the Division of Immunology and Allergy, Children's Hospital of Philadelphia, and the Department of Pediatrics, Perelman School of Medicine at the University of Pennsylvania, Philadelphia; [w]the Louisiana State University Health Sciences Center and Children's Hospital, New Orleans; [x]the Division of Bone Marrow Transplant, Children's Healthcare of Atlanta, Emory University School of Medicine, Atlanta; [y]the Leeds Institute for Rheumatic and Musculoskeletal Medicine, St James University Hospital, Leeds; [z]the Primary Immunodeficiency Group, Institute of Cellular Medicine, Newcastle University, Newcastle upon Tyne; [aa]Oxford University Hospitals NHS Trust and NIHR Oxford Biomedical Research Centre, Oxford; [bb]the Division of Bone Marrow Transplantation and Immune Deficiency, Department of Pediatrics, Cincinnati Children's Hospital Medical Center, University of Cincinnati; the Departments of [cc]Dermatology, [dd]Pediatric Hematology Oncology, and [ee]Pediatrics, University of Alabama at Birmingham; [ff]University of Washington School of Medicine and Seattle Children's Hospital, Seattle.

Background: Caspase activation and recruitment domain 11
(*CARD11*) encodes a scaffold protein in lymphocytes that links
antigen receptor engagement with downstream signaling to
nuclear factor κB, c-Jun N-terminal kinase, and mechanistic
target of rapamycin complex 1. Germline *CARD11* mutations
cause several distinct primary immune disorders in human
subjects, including severe combined immune deficiency (biallelic
null mutations), B-cell expansion with nuclear factor κB and T-
cell anergy (heterozygous, gain-of-function mutations), and
severe atopic disease (loss-of-function, heterozygous, dominant
interfering mutations), which has focused attention on *CARD11*
mutations discovered by using whole-exome sequencing.
Objectives: We sought to determine the molecular actions of an
extended allelic series of *CARD11* and to characterize the
expanding range of clinical phenotypes associated with
heterozygous *CARD11* loss-of-function alleles.
Methods: Cell transfections and primary T-cell assays were used
to evaluate signaling and function of *CARD11* variants.
Results: Here we report on an expanded cohort of patients
harboring novel heterozygous *CARD11* mutations that extend
beyond atopy to include other immunologic phenotypes not
previously associated with *CARD11* mutations. In addition to
(and sometimes excluding) severe atopy, heterozygous missense
and indel mutations in *CARD11* presented with immunologic
phenotypes similar to those observed in signal transducer and
activator of transcription 3 loss of function, dedicator of
cytokinesis 8 deficiency, common variable immunodeficiency,
neutropenia, and immune dysregulation, polyendocrinopathy,
enteropathy, X-linked–like syndrome. Pathogenic variants
exhibited dominant negative activity and were largely confined
to the CARD or coiled-coil domains of the CARD11 protein.
Conclusion: These results illuminate a broader phenotypic
spectrum associated with *CARD11* mutations in human subjects
and underscore the need for functional studies to demonstrate
that rare gene variants encountered in expected and unexpected
phenotypes must nonetheless be validated for pathogenic
activity. **(J Allergy Clin Immunol 2019;143:1482-95.)**

Abbreviations used	
AD:	Atopic dermatitis
BENTA:	B-cell expansion with nuclear factor κB and T-cell anergy
CARD:	Caspase activation and recruitment domain
CC:	Coiled-coil
CVID:	Common variable immunodeficiency
DN:	Dominant negative
GFP:	Green fluorescent protein
GOF:	Gain of function
IPEX:	Immune dysregulation, polyendocrinopathy, enteropathy, X-linked
LOF:	Loss of function
MFI:	Mean fluorescence intensity
mTORC1:	Mechanistic target of rapamycin complex 1
NF-κB:	Nuclear factor κB
TCR:	T-cell receptor
tSNE:	t-distributed stochastic neighbor embedding
WES:	Whole-exome sequencing
WT:	Wild-type

Hypomorphic mutations in genes with protein products that are
critical for immune function provide an opportunity to assess the
protein's roles in the context of a functioning but impaired
immune response. Unlike the unresponsive or absent effector
compartments often associated with null mutations that manifest
as severe combined immune deficiency, these mutations preserve
sufficient function to allow for development of the particular cells
or organs with which it is involved. Studies of such allelic variants
in mice and other model organisms have taught us much about
immune system development and function. With the wider
availability and application of next-generation sequencing tech-
nologies, we now have more opportunities to explore the
phenomenon of allelic variance and phenotypic heterogeneity
in human subjects. One example can be found in the case of
recombination-activating gene 1 *(RAG1)*: null mutants lead to the
absence of T cells and grossly abnormal thymic development.
Hypomorphic mutations lead to functioning T cells but disrup-
tions of repertoire and thymic development that shed light on

immune tolerance, RAG1 protein domain function, and other im-
mune processes.[1]

Another example is found in different types of mutations
described in caspase activation and recruitment domain 11
(CARD11), leading to different phenotypes. CARD11 is a critical
1154-amino-acid protein scaffold best known for linking antigen
recognition with downstream nuclear factor κB (NF-κB) activa-
tion in lymphocytes.[2,3] The protein CARD11 (also known as
CARMA1 and represented by the sequences NP_115791.3 and
NM_032415) includes an N-terminal caspase recruitment domain
(CARD; 1-110), LATCH (112-130), coiled-coil (CC, 130-449)
domains, and a C-terminal membrane-associated guanylate ki-
nase domain (667-1140) comprised of the PDZ, SH3, and GUK
domains. Biallelic null mutations of *CARD11* in both patients
and mouse models lead to severe T- and B-cell immune defi-
ciency.[4] Somatic gain-of-function (GOF) *CARD11* mutations
are commonly found in patients with non-Hodgkin B-cell lym-
phomas, whereas germline GOF mutations give rise to B-cell
expansion with nuclear factor κB and T-cell anergy (BENTA) dis-
ease in human subjects.[2,5,6] Surprisingly, hypomorphic/dominant
negative (DN) mutations in both mice and human subjects permit
sufficient effector function to reveal a strong disposition toward
atopic phenotypes in addition to variable immune deficiency.[7-9]
Because CARD11 oligomerization is essential for downstream
signaling, heterozygous variants can either enhance or domi-
nantly interfere with CARD11 function.[10,11]

Greater access to next-generation sequencing virtually gua-
rantees that variants in a particular gene can now be identified in
patients with ever-broadening phenotypes, especially for cases of
GOF and hypomorphic loss-of-function (LOF) mutations.[12]
Although algorithms can assist in predicting which variants are
likely to be benign or deleterious, previously undescribed rare
or novel variants in such genes must always be validated for path-
ogenicity by using relevant biological assays. Moreover, *in silico*
prediction methods do not distinguish between variants seen in
the heterozygous and homozygous states, which is critical for
CARD11. Furthermore, collection and testing of variants from
as many centers as possible can more accurately determine the

breadth of disease associated with a given gene, especially given the role that referral bias can play in any given center.

Therefore we report our experience with numerous heterozygous mutations in *CARD11* in the context of severe familial atopic disease and other immunologic phenotypes not previously associated with *CARD11* mutations. The atopy described here is a genetic tendency to develop symptoms of immediate hypersensitivity (eg, food allergy and allergic rhinitis) or allergic inflammation (eg, eczema and eosinophilic esophagitis), irrespective of specific allergen sensitization.[13] In many cases rare or novel mutations were uncovered in whole-exome sequencing (WES)/whole-genome sequencing performed at major referral centers for multiple reasons, particularly in patients without a clear putative genetic diagnosis.

Here we attribute several new DN *CARD11* mutations to an expanded list of disease manifestations and describe assays designed to help differentiate pathogenic versus nonpathogenic variants in *CARD11*. Importantly, results of these assays are interpreted within the context of specific genotypic/phenotypic criteria that help to define a differential diagnosis for patients harboring *CARD11* DN mutations. In addition to severe atopy, heterozygous missense mutations in *CARD11* with DN activity can present with common variable immunodeficiency (CVID), neutropenia, cutaneous viral infections, and immune dysregulation, polyendocrinopathy, enteropathy, X-linked (IPEX)–like syndrome. Collectively, our findings define a broader spectrum of immune disease associated with detrimental *CARD11* mutations, which are most often confined to specific domains of the CARD11 protein. Nevertheless, our evaluations underscore the idea that rare gene variants found by using WES/whole-genome sequencing can be pathogenic even when not matching with reported phenotypes. At the same time, *CARD11* mutations associated with an expected phenotype must nonetheless be validated for pathogenic activity by using functional studies.

METHODS
Patients

Informed consent was obtained from all participating patients and their family members according to protocols approved by institutional review and ethics boards at their respective institutions.

WES and genetic analysis

WES was performed in the majority of patients described here, according to established protocols. For example, kindreds 6, 19, and 29 were analyzed as follows. Genomic DNA was extracted from peripheral blood cells, and the Illumina paired-end genomic DNA sample preparation kit (PE-102-1001; Illumina, San Diego, Calif) was used for preparing the libraries, followed by the exome-enriched library with the Illumina TruSeq exome kit (FC-121-1008; Illumina). Samples were sequenced on an Illumina HiSeq as 100-bp paired-end reads. DNA reads were mapped to the GRCh38 human genome reference by using the default parameters of the Burrows-Wheeler Aligner (bio-bwa.sourceforge.net). Single nucleotide substitutions and small insertion deletions were identified and filtered based on quality with SAMtools software package (samtools.sourceforge.net) and annotated with the Annovar tool (www.openbioinformatics.org). Filtering of variants for novelty was performed according to minor allele frequency, mouse mutant phenotype in the homologous mouse gene, Mendelian disease associations (OMIM), pathway analysis (gene ontology), immune system expression (Immgen), CADD, SIFT, and PolyPhen-2 scores.[14-16] After filtering and ranking variants, heterozygous *CARD11* variants were investigated further.

Kindred 14 (R187P) was initially evaluated separately from the other families. Eight samples were subjected to WES, as described previously (see the Methods section in this article's Online Repository at www.jacionline.org).[17] We selected putative causative variants that had an average read depth of 20 or greater and a quality score of 200 or greater and were heterozygous in at least 1 subject. Genetic analysis showed that 7 of the samples were related and 1 sample was not related. The remaining 7 samples were from 1 unaffected subject and 6 affected subjects. We did a combinatorial search for variants present in the heterozygous state in the 6 affected subjects and absent in the unaffected subject. We performed multipoint genetic linkage analysis with Superlink Online SNP,[18,19] assuming a rare disease allele and dominant inheritance. Two variants satisfied the combinatorial condition of being heterozygous in 6 sampled affected subjects and absent in the 1 sampled unaffected subject, MICALL2 (p.Q202*) and CARD11 (p.R187P), and were at the same time located in a region (chromosome 7: 0.0-4.3 Mbp) consistent with genetic linkage.

PBMC signaling analysis

PBMCs were isolated by using Ficoll gradient centrifugation. Phosphorylation of p65 and/or S6 and degradation of IκB were assessed by using intracellular flow cytometry after short *ex vivo* stimulations with phorbol 12-myristate 13-acetate, as previously described.[9] Total PBMCs (10^6/mL) were seeded in 1 mL of RPMI (Gibco, Carlsbad, Calif) supplemented with 10% FBS, penicillin/streptomycin, and L-glutamine in an anti-CD3 antibody (OKT3, 1 μg/mL)–coated 48-well plate to assess S6 phosphorylation under T_H0 conditions. Anti-CD28 antibody (L293, 0.2 μg/mL) and IL-2 (10 ng/mL; PeproTech, Rocky Hills, NJ) were then added to the culture (T_H0), and cells were incubated in a 37°C CO_2 chamber. After 24 hours, cells were pelleted by means of centrifugation, stained with Live/Dead dye (Thermo Fisher, Waltham, Mass), fixed with 1.6% paraformaldehyde in PBS, and then centrifuged and permeabilized with absolute methanol.

Cells were then stained for flow cytometry with fluorochrome-conjugated antibodies after washes with FACS buffer (PBS with 0.5% BSA). The antibodies used for flow cytometry were as follows: CD3 (UCHT1), CD4 (RPA-T4, L200), CD45RA (HI100), and phospho-S6 (N7-548; BD Biosciences, San Jose, Calif). Percentages of phospho-S6$^+$ live CD3$^+$ CD4$^+$ cells gated on the lymphocyte side-scatter and CD45RA compartments are shown.

CARD11 mutant expression plasmids

Modified wild-type (WT) and mutant pUNO-CARD11-FLAG plasmids were constructed and purified, as previously described.[9] Briefly, site-directed mutagenesis was used to introduce single nucleotide variants that were putative point mutations into the WT CARD11 construct (InvivoGen, San Diego, Calif) by using primer-directed linear amplification with Pwo or PfuI polymerase (Roche, Mannheim, Germany), followed by *Dpn*I digestion of methylated template DNA (Thermo Fisher). All inserted variants were confirmed by using Sanger sequencing. All resulting plasmids were purified from DH5α *Escherichia coli* (New England Biolabs, Ipswich, Mass) with a GenElute HP Plasmid Maxi-Prep Kit (Sigma, St Louis, Mo).

Cell transfection assays

Both WT (clone E6.1, ATCC) and CARD11-deficient Jurkat T cells (referred to as JPM50.6 cells) were cultured and transfected as previously described.[9] JPM50.6 cells containing an integrated canonical NF-κB–driven green fluorescent protein (GFP) reporter were originally provided by Dr Xin Lin (MD Anderson Cancer Center, Houston, Tex). Briefly, 5×10^6 Jurkat or JPM50.6 T cells were resuspended in 0.4 mL of RPMI/10% FBS, placed in 0.4-cm cuvettes (Bio-Rad Laboratories, Hercules, Calif), and electroporated (260 V, 950 μF) with 5 to 10 μg of plasmid DNA (BTX; Harvard Apparatus, Holliston, Mass). JPM50.6 cells were stimulated 24 hours after transfection with 1 μg/mL anti-CD3/CD28 antibodies and incubated overnight (BD Biosciences). Relative canonical NF-κB activation in JPM50.6 cells was quantified based on mean fluorescence intensity (MFI)

of an integrated κB-GFP reporter with an Accuri C6 flow cytometer (BD Biosciences).

Cells were washed 24 hours after transfection in PBS and incubated in PBS/1%BSA for 1 hour at 37°C to assess S6 phosphorylation in Jurkat transfectants. After an additional PBS wash, cells were stimulated with 1 μg/mL anti-CD3/CD28 antibodies (BD Biosciences) for 20 minutes at 37°C. Activation was stopped by adding ice-cold PBS, and cells were pelleted and lysed in 1% NP-40 lysis buffer, as previously described.[9]

Lysates (5-10 μg) were separated on 4-20% Tris-Glycine SDS gels and transferred to nitrocellulose membranes (Bio-Rad Laboratories). Membranes were blocked in 5% milk/TBS/0.1% Tween 20 and immunoblotted with the following antibodies: anti–phospho-S6 (Ser235/236), anti-S6 (5G10), anti-CARD11 (1D12, Cell Signaling Technology, Danvers, Mass; LS-C368868, LifeSpan Biosciences, Seattle, Wash; and OASG00985, Aviva Systems Biology, San Diego, Calif), anti-HA (2-2.2.14, Thermo Fisher), anti-FLAG (M2), and anti–β-actin (AC-15, Sigma). Blots were washed 3 times in TBS/0.1% Tween 20, incubated in horseradish peroxidase–conjugated secondary antibodies (SouthernBiotech, Birmingham, Ala), and washed again. Bands were visualized by means of enhanced chemiluminescence (Thermo Fisher) and imaged on a ChemiDoc system (Bio-Rad Laboratories). Spot densitometric quantification of phospho-S6 versus total S6 was performed with ImageLab software (Bio-Rad Laboratories).

Hierarchical clustering analysis

Hierarchical clustering with a complete linkage algorithm and an asymmetric binary distance measure (for binary variables) was used to explore the data contained in Table E1 in this article's Online Repository at www.jacionline.org. Primarily because of a significant proportion of missing data across many of the variables, only a subset of variables was included in the clustering algorithm. Moreover, only subjects with complete data on the chosen subset were included in the hierarchical clustering. Models were also run using different variable sets, distance measures, and clustering algorithms, and this led to different sets of clusters. Hence presented results should be considered exploratory and descriptive.

Unsupervised patient clustering

To depict patients with their phenotypic attributes in 2-dimensional space, we used Gower distance transformation (as implemented in the daisy function in the R cluster v2.0.7-1 package),[20-22] which handles data sets with missing data points, followed by t-distributed stochastic neighbor embedding (tSNE),[23] as implemented in the Rtsne v0.13 library (by using the settings theta = 0 and perplexity = 10). Next, we divided the patient cohort into 3 clusters by using K-means clustering in R (K = 3). The process of using tSNE and K-means to cluster patients was repeated over 10 trials, and consensus assignment was used to assign each patient to a final cluster ID.

To identify phenotypes important for each cluster, we performed attribute selection and logistic regression in Weka v3.8.2.[24] For attribute selection, we used the Fast Correlation-based Feature Search method[25] to select nonredundant attributes. Using the selected attributes, we performed multinomial logistic regression using the SimpleLogistic function[26] with 5-fold cross-validation to build a classifier for assigning patients to one of the 3 clusters. The features selected along with their predicted coefficients allowed us to assess the importance of phenotypes for each class separately. Based on 10 randomized trials, the classifier demonstrated an overall accuracy of 88.1% with an SD of ±11.7%. Sensitivity and specificity for the trials were 98.33% ± 8.42% and 93.90% ± 11.03%, respectively.

Statistics

For JPM50.6 cell transfections, 2-way ANOVAs with Sidak correction were used to compare GFP MFI between WT and mutant CARD11. Phospho-S6/total S6 protein densitometric ratios were normalized to WT values and compared by using a Wilcoxon signed-rank test. For primary cell assays, experimental and technical replicates were limited by the small numbers of patient samples available. For patients in kindreds 6, 19, and 29, ratios of phospho-S6 geometric MFI (stimulated/unstimulated) were compared with those in healthy control subjects (matched per experiment) by using a Kruskal-Wallis test.

RESULTS

Novel DN *CARD11* mutations detected in a broad spectrum of immune disorders

Rare or novel *CARD11* mutations were identified by allergy and primary immunodeficiency referral centers in patients with immune-deficient or dysregulatory phenotypes (Table I). A total of 48 new patients in 27 families with 26 different heterozygous germline *CARD11* variants were referred. Salient patient phenotypes, combined with those already reported,[7,9] are summarized in Tables I and II. These alleles were then evaluated at centers specializing in CARD11 biology and associated diseases and pathways.

First, we investigated whether each variant altered T-cell receptor (TCR) signaling. Each *CARD11* variant was cloned into an expression construct and transfected into WT Jurkat or CARD11-deficient Jurkat (JPM50.6) T-cell lines. As a control, we also tested a variant (p.C150L) identified as a somatic reversion mutant that restored NF-κB signaling in T cells from a CARD11-deficient patient with Omenn syndrome.[27] Upon CD3/CD28 stimulation of transfected JPM50.6 cells, 14 of 26 mutants demonstrated significantly reduced NF-κB activation, indicating LOF (Fig 1, *A*). Two variants (p.P495S and p.R848C) displayed enhanced NF-κB activation only after stimulation; unlike BENTA-associated mutations, these variants did not induce constitutive NF-κB activity.

Because all variants were heterozygous, we next tested whether each LOF mutants could dominantly interfere with WT CARD11 signaling when coexpressed at 50:50 ratios. Among 14 LOF mutations, DN activity (defined as significantly reduced NF-κB activation relative to 100% WT expression) was observed for 10 (Fig 1, *B*). Most of these new DN variants were confined to the CARD domain and proximal CC domains, which are critical for both CARD11 oligomerization and BCL10-MALT1 interactions.[28,29] All variants were comparably expressed in transfected cells, suggesting none of the mutations tested affected CARD11 protein translation and stability (Fig 1, *C*, and data not shown). Although a faint 15-kDa band was noted on prolonged blot exposure, we could not definitively confirm the presence of a truncated K143X protein by means of immunoblotting with available N-terminus specific CARD11 antibodies, which cross-reacted with many nonspecific proteins (data not shown). However, the fact that expression of this construct and not the Q945X truncation mutant[9] exhibits DN activity strongly suggests that it is expressed. Moreover, a K143X CARD11 expression construct engineered to include a C-terminal HA-tag was clearly expressed in JPM50.6 transfectants and exhibited comparable DN activity compared with the untagged form (see Fig E1 in this article's Online Repository at www.jacionline.org).

CARD11 also affects TCR-induced mechanistic target of rapamycin complex 1 (mTORC1) activation.[30,31] Therefore we further tested whether selected *CARD11* variants could disrupt TCR-induced mTORC1 activation by measuring ribosomal S6 protein phosphorylation using immunoblotting. For most mutations within the CARD domain, we observed a trend toward decreased phospho-S6 levels (Fig 1, *C* and *D*), similar to those seen in previously characterized DN mutants.[9] However, these

TABLE I. Clinical phenotypes for all patients with *CARD11* variants

Kindred	Mutation	Genotype	Functional defect	No. of patients	AD	Asthma	Food allergy	Pneumonia	Bronchiectasis	Molluscum contagiosum	Cutaneous HSV	Warts	Other phenotypes
1	R30G	c.88C>G	DN	6	1	3	0	1	0	2	0	0	Bacterial sinusitis/meningitis, visceral leishmaniasis, severe vernal keratoconjunctivitis, florid EoE, severe oral ulcers
2	R30Q	c.89G>A	DN	1	0	0	1	0	0	0	1	0	Bullous pemphigoid
3	R30Q	c.89G>A	DN	2	2	1	2	2	0	2	0	2	Viral pneumonia, *Staphylococcus aureus* skin infection, flu, constipation
4	R30W	c.88C>T	DN	1	1	0	0	0	0	0	0	0	IPEX-like, FTT
5	R30W	c.88C>T	DN	4	3	4	4	3	1	0	0	0	recurrent respiratory tract infections, oral candidiasis, lichen sclerosis of vulva, psoriasis, impetigo
6	R47H	c.140G>A	DN	3	1	1	0	0	0	3	3	3	Neutropenia, LGL
7	R47H	c.140G>A	DN	1	1	1	0	1	0	1	0	1	Progressive hypogammaglobulinemia
8	E57D	c.171A>C	DN	2	2	2	1	2	0	1	0	0	Ulcerative colitis, stroke, peripheral T lymphoma
9	R72G	c.214C>G	DN	2	2	2	0	1	1	0	0	1	Alopecia, joint pain, oral ulcers, pulmonary TB
10	R72G	c.214C>G	DN	1	1	1	0	1	0	1	0	0	Persistent skin infections (VZV, HPV), EBV viremia, progressive B-cell lymphopenia, frequent OM
11	R75Q	c.224G>A	DN	1	0	0	0	0	0	1	0	0	Neutropenia
12	L92W	c.275T>G	DN	1	1	0	0	0	0	0	1	0	
13	K143X	c.427A>T	Weak DN	1	1	0	0	0	0	0	0	0	ITP, alopecia, EoE
14	R187P	c.560G>C	DN	10	10	5	4	4	2	8	6	5	Alopecia, cutaneous vasculitis, mycosis fungoides, broad nose, retained teeth, shingles
15	dup183-196	c.701_713insT	DN	3	3	1	0	3	1	2	1	0	Prominent forehead, broad nose, poor dentition, pulmonary TB, eosinophilic coloproctitis
16	L194P	c.581T>C	DN	1	1	1	1	0	0	1	0	0	
17	V195L	c.583G>C	LOF	1	1	1	0	0	0	0	0	0	Diverticulitis, T2D
18	K362E	c.1084A>G	LOF	1	0	0	0	0	0	0	0	0	Healthy
19	R408H	c.1223G>A	LOF	1	0	0	0	1	0	0	0	0	Evan syndrome, anhidrosis
20	P495S	c.C>T	Hypermorphic w/ TCR stim	1	0	0	0	1	0	0	0	0	IPEX-like, FTT, T1D, alopecia, skin tags
21	I544L	c.1630A>C	Nil	1	1	0	0	0	0	0	0	0	AD
22	R608H	c.1823G>A	Nil	1	1	0	0	0	0	0	0	0	CMV myocarditis, adenoviral hepatitis
23	V659M	c.1975G>A	Nil	1	0	0	0	1	0	0	0	0	Recurrent sinopulmonary/skin infections
24	T670M	c.2009C>T	Nil	1	0	0	0	0	0	0	0	0	Seizures, mental retardation, TB, candidiasis, facial dysmorphism
25	E766D	c2298G>T	Nil	1	1	0	0	0	0	0	0	0	Severe AD
26	R848C	c.2542C>T	Hypermorphic w/ TCR stim	2	1	1	0	1	0	0	0	0	AHA, ITP, refractory cytopenias, drug-induced lupus, Crohn disease
27	R912Q/ D1152N	c.2735G>A, c.3454G>A	Nil	1	0	0	0	1	0	0	0	0	Late-onset recurrent sinopulmonary infections
28	S923L	c.2768C>T	LOF	1	0	0	0	1	0	0	0	0	Agammaglobulinemia, giardiasis

(Continued)

TABLE I. (Continued)

Kindred	Mutation	Genotype	Functional defect	No. of patients	AD	Asthma	Food allergy	Pneumonia	Bronchiectasis	Molluscum contagiosum	Cutaneous HSV	Warts	Other phenotypes
29	R974C	c.2920C>T	Weak DN	2	0	1	0	1	0	1	0	0	Neutropenia, mycobacterial disease
30	R975W	c.2923C>T	DN	2	2	1	1	0	0	0	1	0	
31	V983M	c.2947G>A	Nil	2	1	1	1	1	0	0	1	0	
32	E1028K	c.3082G>A	Nil	1	0	0	0	0	0	0	0	0	sJIA, MAS, pheochromocytoma, migraines
		DN	13	44	32	24	14	19	5	23	13	12	
		%			73%	55%	32%	43%	11%	52%	30%	27%	
		Non-DN	15	16	6	3	1	7	0	0	1	0	
		%			38%	19%	6%	44%	0%	0%	6%	0%	
		TOTAL	28	60	38	27	15	26	5	23	14	12	

Kindreds are listed in the order each variant appears within the CARD11 protein.

AHA, Autoimmune hemolytic anemia; *EoE*, eosinophilic esophagitis; *FTT*, failure to thrive; *HPV*, human papillomavirus; *ITP*, idiopathic thrombocytopenic purpura; *LGL*, large granular lymphocytic leukemia; *MAS*, macrophage activation syndrome; *sJIA*, systemic juvenile arthritis; *TB*, tuberculosis; *T1D*, type 1 diabetes; *T2D*, type 2 diabetes; *VZV*, varicella zoster virus.

differences did not reach statistical significance because of the inherent variation in our assays. mTORC1 signaling is exquisitely sensitive to subtle perturbations in cell viability, culture media contents, and stimulation conditions, particularly in Jurkat T cells (K. Hamilton, personal communication). Interestingly, some mutants (eg, p.R72G and p.R187P) had no appreciable effect on TCR-induced S6 phosphorylation despite impaired NF-κB activation in Jurkat transfectants (Fig 1, *C* and *D*). Collectively, these transfection results suggest that *bona fide* DN mutations in *CARD11*, which are often located in the CARD domain, attenuate TCR-induced NF-κB activation with variable effects on mTORC1 signaling (Fig 1, *E*).

Patient phenotypes with DN *CARD11* mutations

We compared a total of 60 patients from 32 kindreds carrying heterozygous *CARD11* variants (Table I). Including those previously published,[7,9] we identified 28 distinct *CARD11* alleles, of which 14 are DN, as determined by using the functional assays described above. All kindred pedigrees with confirmed *CARD11* DN variants are shown in Fig 2. All patients were referred with immunologic phenotypes for investigation, typically presenting in childhood. Therefore we compared manifestations in those with functional *CARD11* DN defects with those in patients with no obvious DN functional defect, even if hypomorphic (Tables I and II). Severe atopic dermatitis (AD) was present in most patients with DN mutations (32/44 [73%]), compared with non-DN variants (5/16 [31%]). Other atopic symptoms were noted in patients with DN variants, including asthma (55%) and food allergies (32%) and, less frequently, rhinitis and eosinophilic esophagitis (Table I). Cutaneous viral infections were also more common in patients with DN alleles, including molluscum contagiosum (52%), cutaneous herpes simplex virus 1 infection (30%), and warts (27%; Table I). We also observed cases of neutropenia and presentations similar to other syndromes associated with increased IgE levels and infections (kindred 14), including IPEX-like syndrome (kindred 4), in patients with functional DN alleles but not in others. Of note, the patient with an IPEX-like presentation (including failure to thrive, bloody diarrhea, and severe eczema) carried the identical mutation (p.R30W) as described recently by Dadi et al[7] (kindred 5) in a family with severe atopy, infection, and

TABLE II. Clinical summary of patients with *CARD11* DN mutations

Age (mean ± SD)	23.3 ± 19.5
Age of disease onset (mean ± SD)	5.2 ± 6.7
Female sex	50%

Clinical phenotype	Patients affected
Atopic disease	89%
AD	73%
Asthma	55%
Food allergies	32%
Eosinophilic esophagitis	7%
Cutaneous viral infections	68%
Respiratory tract infections	68%
Autoimmunity	20%
Neutropenia	14%
Oral ulcers	14%
Hypogammaglobulinemia	11%
Lymphoma	7%

The table shows mean age, sex ratio, and relevant phenotypes shared by patients with *CARD11* DN mutations, with the percentage of affected patients shown for each category.

mild (late-onset) autoimmunity. Prominent phenotypes in the collective cohort of patients with *CARD11* DN mutations are summarized in Table II. In addition to atopic disease (89%), significant viral skin infections (68%) and lung diseases (eg, infections, pneumonia, and bronchiectasis; 68%) were the most prominent symptoms shared by patients harboring DN *CARD11* mutations (Table II). Additional phenotypes included autoimmunity (20%), most commonly alopecia but also including idiopathic thrombocytopenic purpura and bullous pemphigoid. Neutropenia was also observed in 5 (14%) patients (including 4 with no demonstrable atopic disease), although an autoimmune cause could not be confirmed. Oral ulcers were also observed (14%) and might be linked to neutropenia. Four patients had lymphoproliferative disease (large granular lymphocytic leukemia, peripheral T-cell lymphoma, and/or mycosis fungoides). Notably, 3 patients from 2 families had little to no atopic disease (1 had a mild IgE levels increase without clinical manifestations) but did have neutropenia with humoral defects including progressive B-cell lymphopenia, poor class-switched
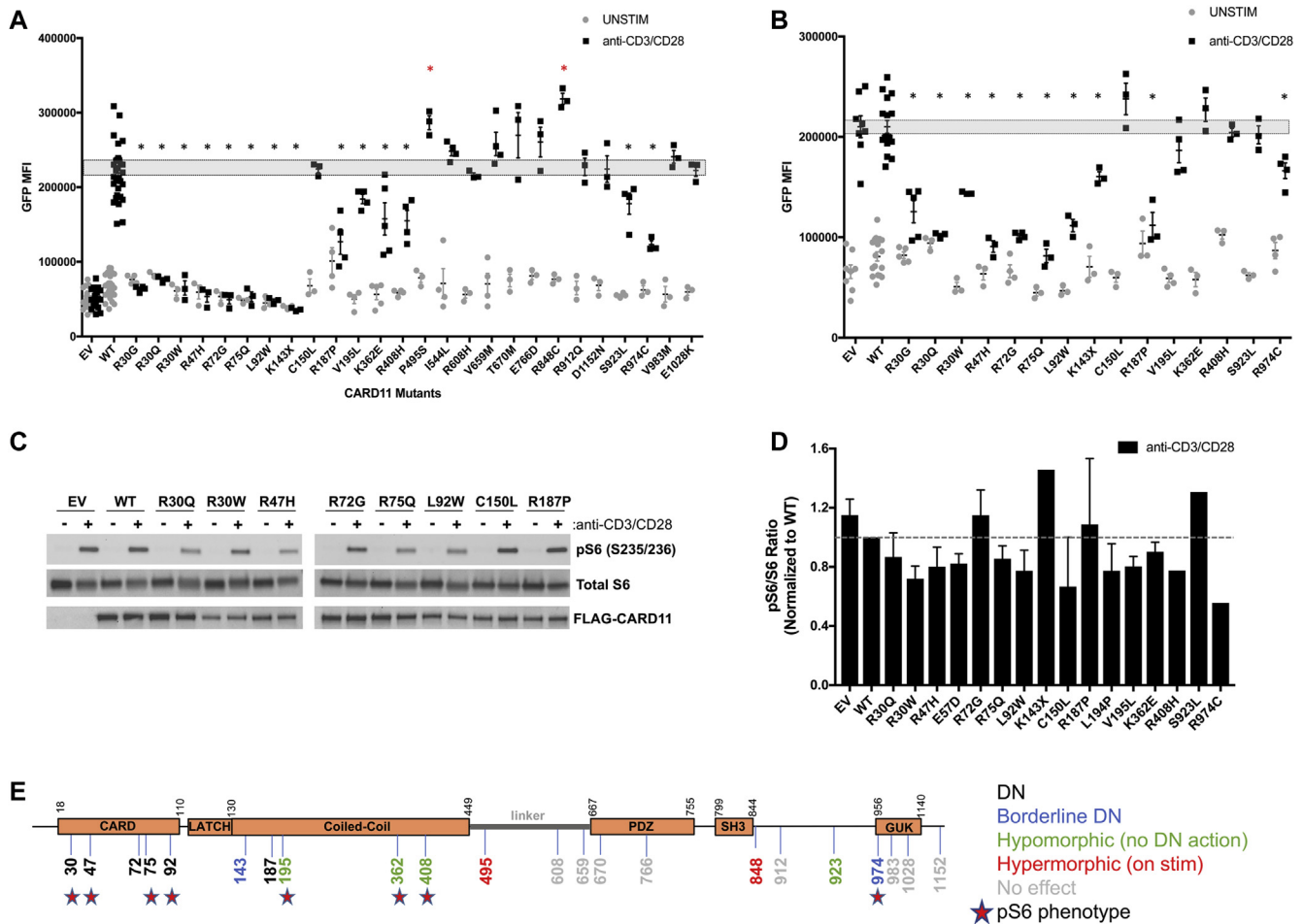
FIG 1. Jurkat T-cell transfection screens for LOF/DN activity of new CARD11 variants. **A,** Quantification of NF-κB–induced GFP reporter activity in CARD11-deficient JPM50.6 T cells transfected with empty vector *(EV)*, WT, or mutant CARD11 constructs and subsequently stimulated with anti-CD3/CD28 antibodies. Data are means ± SEMs for 3 or more separate transfections each. **B,** Quantification of NF-κB–induced GFP in JPM50.6 cells transfected with equal ratios of WT and mutant CARD11 constructs. Data are means ± SEMs for 3 or more separate transfections of each LOF variant. *Dashed boxes* in Fig 1, *A* and *B*, indicate SEMs for numerous WT transfections. *Asterisks* denote statistically significant reductions in GFP MFI versus WT (Fig 1, *A*) or WT+WT CARD11 (Fig 1, *B*) after stimulation, indicating DN activity (*P* < .05). **C,** Immunoblot for phospho-S6, total S6, and FLAG-CARD11 expression in Jurkat T cells transfected with CARD11 constructs with or without 20 minutes of stimulation with anti-CD3/CD28 antibodies. Data are representative of several independent experiments. **D,** Spot densitometric quantification of phospho-S6/ S6 ratio for each mutant normalized to WT (*dashed line* = 1). Data are means ± SDs for 2 to 3 experiments for each variant. **E,** Schematic diagram of CARD11 protein including new DN, LOF, hypermorphic, and benign (ie, no effect) variants. *Stars* indicate mutations with reduced phospho-S6 levels in Fig 1, *D*.

B-cell memory, and antibody deficiency. Indeed, low IgM levels and impaired humoral responses to certain vaccines (eg, pneumococcal) were observed in several patients. Relevant immunologic phenotypes, including total and specific antibody defects and lymphocyte subsets, are summarized in Table III and Table E1 in this article's Online Repository at www. jacionline.org.

Hierarchical clustering with a complete linkage algorithm and an asymmetric binary distance measure was used to explore the cohort for specific phenotypic patterns for patients (n = 36) and phenotypes (n = 7) for which phenotypic data were more complete. Although the small size of the cohort precludes any assessment of statistical significance, descriptively we saw (1) a cluster of neutropenic patients with low IgM and lower IgE levels,

(2) patients with AD and asthma who had low IgM levels, (3) patients with AD without asthma who had low IgG and low IgA levels, and (4) patients with high IgA levels, normal IgM levels, lack of neutropenia, and IgE levels that tracked with the presence of AD (see Fig E2, *A*, in this article's Online Repository at www. jacionline.org). These clusters did not appear to correlate with specific mutations.

To be more inclusive of phenotypes with some missing data, we performed an additional analysis using all phenotypes (n = 31) and patients (n = 44). Data were transformed into a Gower distance matrix and reduced to 2 dimensions by using tSNE before applying K-means clustering to partition the patients into three clusters. Fig E2, *B*, summarizes phenotypic characteristics of each cluster. Interestingly, cluster 2 was
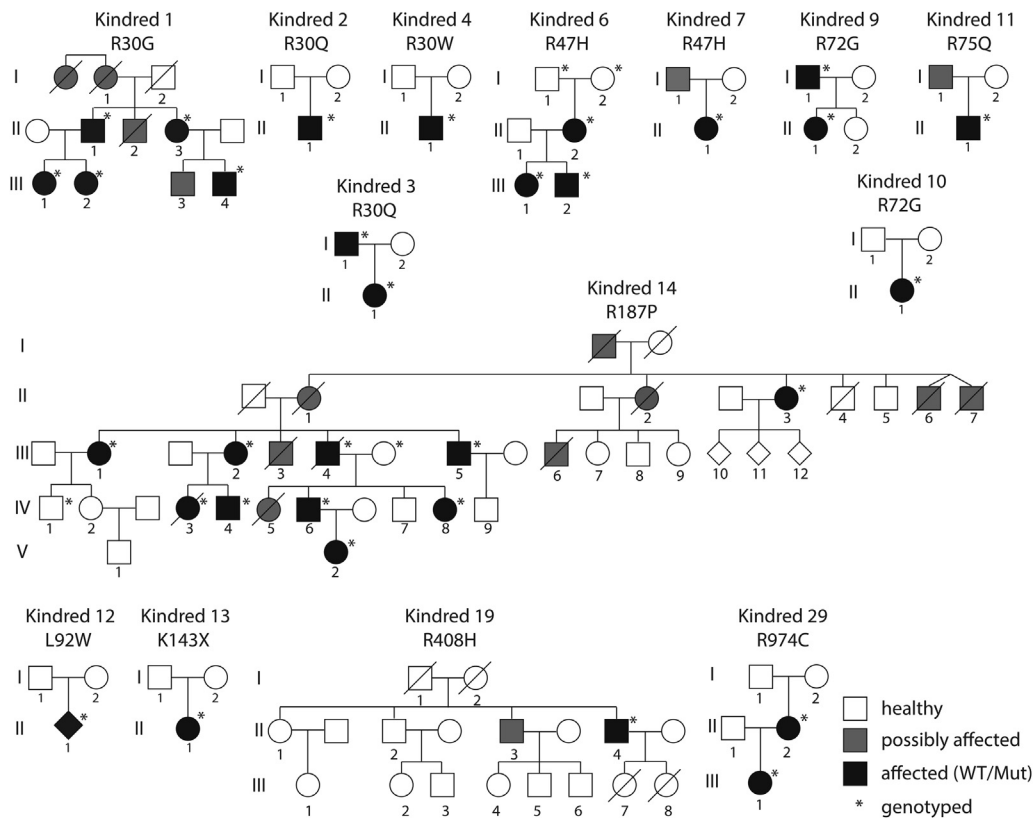
FIG 2. Pedigrees for new CARD11 DN variants. The key indicates healthy (white), affected (symptomatic with confirmed heterozygous DN mutation), and possibly affected (symptomatic, no genotype available). *Asterisks* denote patients who were definitively genotyped.

characterized by lack of AD, skin bacterial infections, pneumonia, and allergic rhinitis but included patients with neutropenia and abnormal IgM and IgA levels. This cluster included all patients with R30G and R974C, most patients with R47H, and the single patient with R75Q mutations. Again, all phenotypic correlations predicted by these clusters are merely descriptive for this limited patient cohort.

The largest family analyzed included 10 patients from the United Kingdom (kindred 14) who presented with autosomal dominant inheritance of symptoms typically associated with dedicator of cytokinesis 8 deficiency, including increased serum IgE levels with significant atopic disease, recurrent respiratory tract infections, skin abscesses, and recurrent or persisting viral skin infections, such as molluscum contagiosum, herpes infections, or warts (Fig 3 and Table I). Additionally, 2 patients had mycobacterial complications. Surprisingly, mild skeletal/connective tissue abnormalities characteristic for the signal transducer and activator of transcription 3 DN autosomal dominant HIES were also observed in 6 of 10 affected family members. Patient III.4 died from disseminated mycosis fungoides. Immune phenotyping of patients' PBMCs from this family revealed low $CD8^+$ T-cell numbers and high $CD4^+$ T-cell numbers, with a shift toward the naive compartment and reduction of memory $CD4^+$ T cells. The B-cell compartment was normal.

Flow cytometric analyses of other patients, when available, often showed B-cell defects, including low total/memory B-cell counts in those with specific antibody deficiency and low IgM levels in several patients (Table III). Other assays performed showed diminished mitogen-induced T-cell proliferation in the majority of patients tested and relatively normal frequencies of regulatory T cells, as previously reported (Table III). Detailed clinical and laboratory findings for individual patients, where available, are included in Table E1.

Primary cell signaling defects in CARD11 DN lymphocytes from patients

In 7 of the patients with confirmed DN mutations, primary cells were available for evaluation of NF-κB signaling by using short phorbol 12-myristate 13-acetate activation. Hallmarks of TCR-induced canonical NF-κB activation, including p65 phosphorylation and IκBα degradation, were impaired in all samples tested (Fig 4). Impaired upregulation of activation markers at 24 hours and skewed cytokine secretion was also noted in multiple $CD4^+$ T-cell samples from patients, which is consistent with previous findings (see Figs E3 and E4 in this article's Online Repository at www.jacionline.org). Of note, NF-κB activation in lymphocytes from the patient with the V195L substitution, which was LOF but did not show DN activity in our transfection system, was also abnormal. Because haploinsufficiency does not likely lead to direct DN activity,[9] the result suggests either that other lesions explain the cellular and clinical phenotype or that the effects of this mutation on the pathway are not revealed by using our transfection system. The variability in phospho-S6 activation in the primary cell assay precludes making a definitive conclusion regarding its utility, although small

TABLE III. Immunologic phenotypes for patients with *CARD11* DN variants

Kindred	Mutation	No. of patients	T-cell proliferation defect	Specific antibody response defect	Total antibody defect	Total CD4	Memory CD4	Total CD8	Memory CD8	Total B cells	Low CS/memory B cells	NK cells	Treg cells	IgE	Eosinophils
1	R30G	6	No	Yes (2/6)	No	Normal	ND	Normal	ND	Normal	Normal	Normal	ND	High (3/6)	High (2/6)
2	R30Q	1	Yes	Yes	Yes (low IgM)	Normal	Normal	Normal	Normal	Borderline low	ND	Borderline low	ND	High	High
3	R30Q	2	Yes (2/2)	Yes (2/2)	Yes (2/2)	Normal	Normal	Normal	Normal	Normal	Low	Normal	ND	High (2/2)	High (1/2)
4	R30W	1	Unknown	Unknown	Unknown	Unknown	Unknown	Unknown	Unknown	Unknown	Unknown	Unknown	Low	High	ND
5	R30W	4	Yes (4/4)	Yes (2/4)	Yes (2/4)	Normal	ND	Normal	ND	Low (1/4)	ND	Normal	ND	High	High (3/4)
6	R47H	3	Yes (3/3)	Yes (2/2)	Yes (1/3)	Normal	Low (3/3)	Normal	Low (3/3)	Normal	Low (3/3)	Normal	Normal	High 1/3	Normal
7	R47H	1	Yes	Yes	Yes	Normal	Low	Normal	ND	Low	Low	Normal	Normal	High	Normal
8	E57D	2	Yes (1/2)	Unknown	Yes (1/1)	Normal	ND	Normal	ND	Normal	Normal	Low (1/2)	Normal	High	High
9	R72G	2	Yes (1/2)	Yes (2/2)	No	Normal	ND	Normal	ND	Low (1/2)	Absent	Normal	ND	ND	ND
10	R72G	1	No	Yes	No	High	Normal	High	Normal	Low	Normal	Normal	Normal	High	High
11	R75Q	1	Yes	Yes	No	Normal	Normal	Normal	Normal (high TEMRA)	Low	Low	Low	Low	Normal	Normal
12	L92W	1	ND	No	Yes	Normal	Normal	Normal	Normal	Normal	Normal	Normal	Normal	High	ND
13	K143X	1	ND	Yes	Yes	Normal	Normal	Normal	Normal	Normal	Normal	Normal	Normal	Normal	Normal
14	R187P	10	ND	Yes (2/10)	Yes (1/10)	High (3/3)	Low (3/3)	Low (1/3)	ND	Low (1/3)	Low (1/3)	Low (3/4)	Normal	High (0/3) (8/10)	High (8/10)
15	dup183-196	3	Yes (3/3)	No	No	Normal	ND	Normal	ND	Low (1/3)	ND	Normal	Normal	High	High
16	L194P	1	Yes	Yes	No	Normal	Borderline low	Normal	Borderline low	Normal	Normal	Normal	Normal	High	High
29	R974C	2	No	Yes (2/2)	IgA (1/2)	Normal	Normal	Normal	Normal	Normal	Normal	Normal	Normal	Normal	Normal
30	R975W	2	Yes (1/2)	No	No	Normal	Borderline low (1/2)	Normal	Normal	Normal	Normal	Borderline low	Normal	High	High
	Total	44	61% (19/31)	49% (20/41)	29% (12/42)										

Descriptors are based on institution-specific reference ranges for each parameter (see Table E1) as follows: *absent*, no cells detected; *Low*, more than 10% below reference range minimum; *Borderline low*, within 10% of reference minimum; *High*, more than 10% above reference range maximum. Numbers in parentheses indicate the number of patients with the observed defect/number of patients tested within each kindred.

CS, Class switched; *ND*, not determined; *TEMRA*, T effector memory CD45RA$^+$ cells; *Treg*, regulatory T.

but reproducible defects were observed in 4 patients tested from kindreds 6 and 19 (Fig 5, *A* and *B*). Moreover, we noted a more reproducible diminution of phospho-S6 could be observed in samples from patients with CARD11 DN mutations activated for 24 hours (Fig 5, *C*).

DISCUSSION

In this report we describe multiple new DN *CARD11* mutations associated with additional immunodeficient and dysregulatory conditions in human patients. Recent reports identified DN *CARD11* mutations in a handful of patients presenting with severe AD and other allergic conditions with or without additional infections.[7,9] The substantially larger cohort assembled here illuminates a broader phenotypic spectrum of disease tied to *CARD11* DN mutations, including frequent sinopulmonary infections, cutaneous viral infections, neutropenia, hypogammaglobulinemia, and lymphoma (Table II). Atopic disease was the cardinal feature noted in most patients (89%), frequently presenting in childhood as AD but also including asthma, allergic rhinitis, food allergies, and even eosinophilic esophagitis (Table II). However, atopy was mild or absent in a number of patients examined in this report, with no measured differences in TCR-driven signaling responses. There were no obvious clinical similarities between nonatopic patients with CARD11 DN mutations beyond

neutropenia (present in 4 patients). It is possible that atopic symptoms improved over time for some older adults for whom a detailed clinical history was lacking, similar to previously described patients.[9] Furthermore, unrelated patients with the same mutation (eg, R30Q and R72G) and even family members harboring identical mutations (eg, p.R47H and p.R187P) demonstrated differences in both the variety and severity of disease symptoms. From our characterization of this expanded patient cohort, we conclude that *CARD11* DN mutations exhibit high penetrance and variable expressivity for several phenotypes that can extend beyond atopy. Other genetic variants or polymorphisms could certainly be influencing the heterogeneity and severity of phenotypes observed in certain patients.

Lack of atopic disease in patients with biallelic *CARD11* null mutations, which are rarely associated with severe combined immune deficiency, is likely due to the relative lack of lymphocyte effector function.[32,33] However, the absence of atopy observed in certain patients described here with *CARD11* DN mutations, all of whom had lived into adulthood without major intervention, is surprising. Interestingly, unsupervised clustering analyses identified a subset of these patients from 4 kindreds that presented with neutropenia, abnormal immunoglobulin levels, and fewer skin/respiratory tract infections (Fig E2), although the significance of these associations cannot be formally assessed within this limited cohort. We otherwise noted no
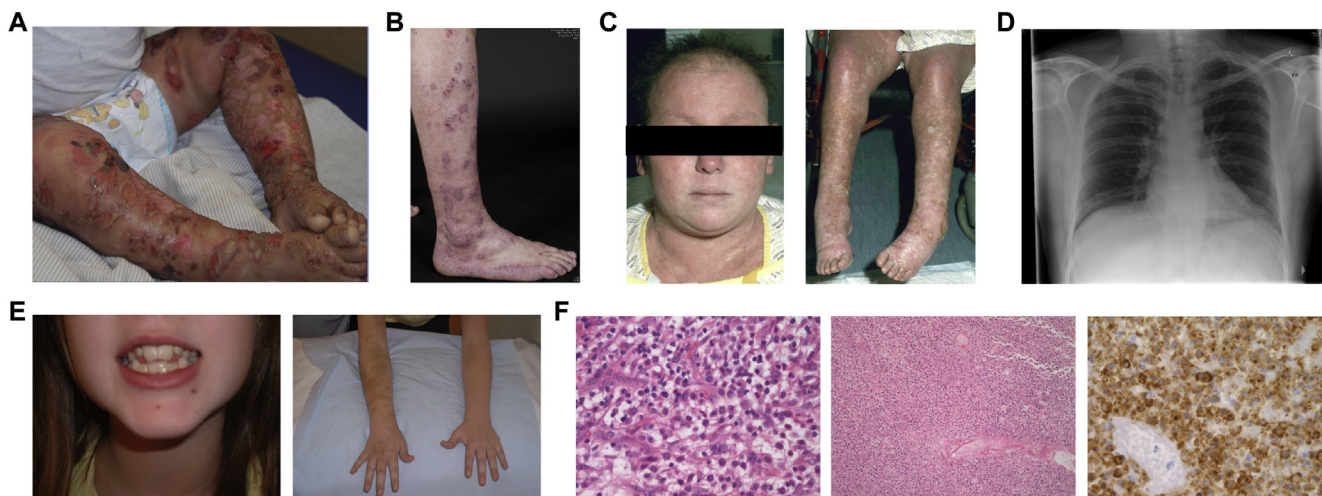
FIG 3. Clinical presentation of patients with DN CARD11 mutations: R30Q (kindred 2; **A**) and R187P (kindred 14; **B-F**). Fig 3, *A*, Patient II.1 displaying herpes simplex virus 1 *(HSV-1)* skin disease. Fig 3, *B*, Patient IV.6 displaying severe eczema. Fig 3, *C*, Cutaneous vasculitis (both) and alopecia (left) in patient IV.3. Fig 3, *D*, Chest radiograph of patient III.5 from 2008 depicting bronchiectasis. Fig 3, *E*, Abnormal dentition *(left)* and brachial hypermelanosis *(right)* in patient IV.8. Fig 3, *F*, Histologic findings in patient III.4 with cutaneous T-cell lymphoma (mycosis fungoides). *Left*, Viable pleomorphic blasts ×40; *middle*, necrotic lymph node replaced by lymphoma at low power; *right*, CD2 staining viable and semiviable cells.
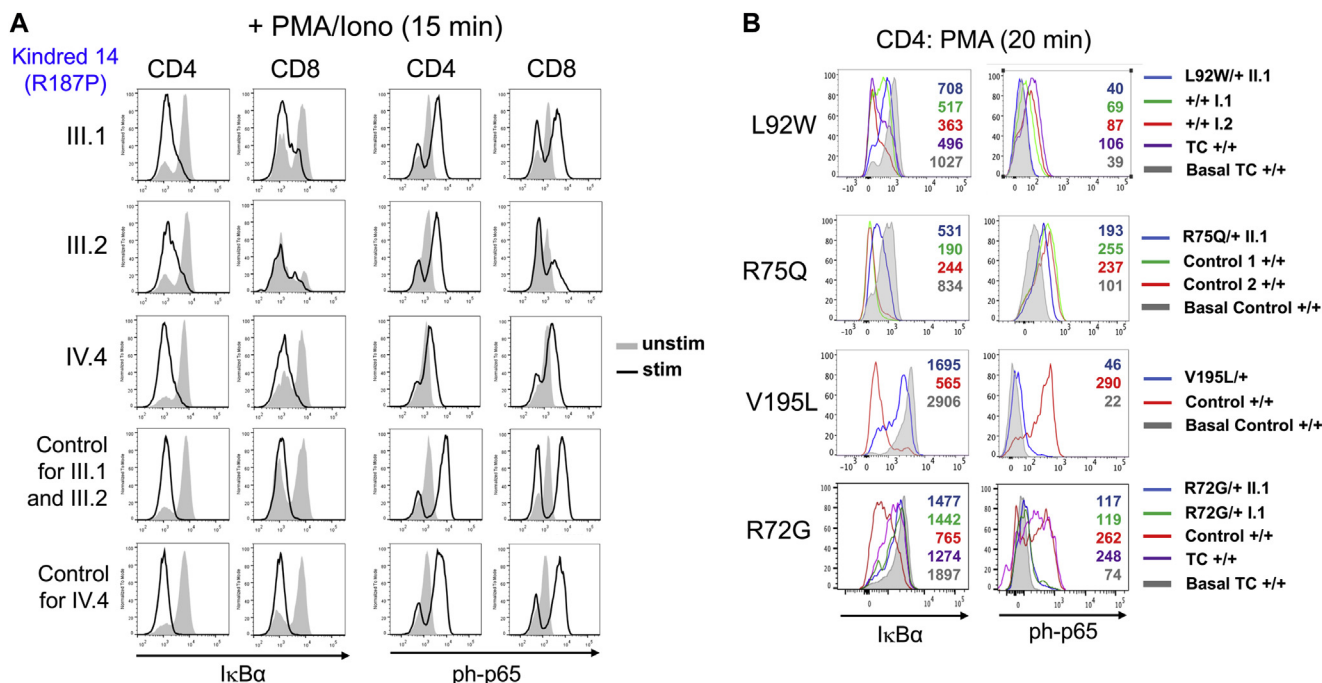
FIG 4. Defective NF-κB activation in primary T cells from patients with CARD11 DN/LOF mutations. **A,** Primary CD4$^+$ and CD8$^+$ T cells from 3 kindred 14 patients (III.1, III.2, and IV.4) and 2 control subjects were left unstimulated *(gray histograms)* or stimulated for 15 minutes with phorbol 12-myristate 13-acetate *(PMA)* plus ionomycin *(Iono; black histograms)*. IκB degradation and p65 phosphorylation was detected by using intracellular flow cytometry. **B,** Total PBMCs from affected patients, unaffected family members, and control subjects (labeled at right, + = WT) were stimulated for 20 minutes with PMA or left unstimulated (basal: *gray histograms*). IκB degradation and p65 phosphorylation were detected in gated CD4$^+$ T cells by using intracellular flow cytometry. Geometric MFI *(gMFI)* values are listed within each histogram.

particular genotype/phenotype correlations, nor were there patterns of other comorbid conditions that suggested substantially different phenotypic manifestations. Phenotypic variation within families suggests that other genetic variants, which might not be pathogenic by themselves, or differences in environmental exposures could influence the phenotype. As more *CARD11* variant patients are found, demographic patterns might be possible to establish.
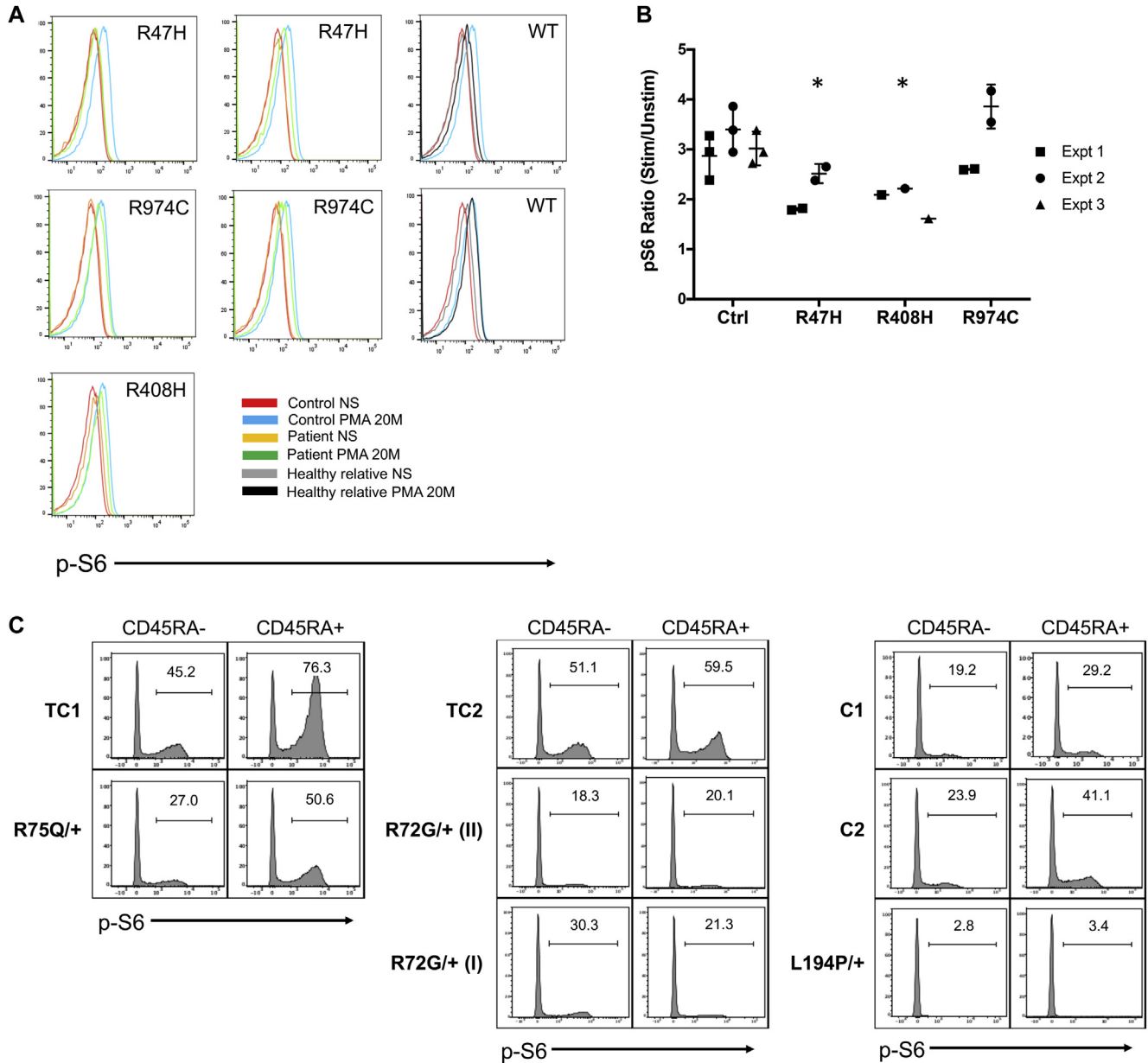
FIG 5. Defective S6 phosphorylation in primary T cells from affected patients with CARD11 DN mutations after acute and prolonged stimulation. **A,** Primary CD4$^+$ T cells from affected patients in kindreds 6, 19, and 29; healthy relatives; and control subjects were not stimulated *(NS)* or stimulated with phorbol 12-myristate 13-acetate *(PMA)* for 20 minutes. S6 phosphorylation was measured by using intracellular flow cytometry. **B,** The ratio of phospho-S6 gMFI for stimulated versus unstimulated cells is plotted for each of 3 experiments represented in Fig 6, *A*. *Asterisks* denote statistical significance relative to control subjects ($P < .05$, Kruskal-Wallis test). **C,** Total PBMCs from affected patients with CARD11 DN mutations, control subjects *(C)*, and travel control subjects *(TC)* were cultured under T$_H$0 conditions for 24 hours. S6 phosphorylation was measured in CD4$^+$CD45RA$^-$ or RA$^+$ cells gated for high versus low side scatter *(SSC)* by using intracellular flow cytometry; percentages of phospho-S6$^+$ cells are labeled within each histogram.

Nonatopic phenotypes associated with *bona fide* DN mutations shed new light on important biological functions governed by CARD11 signaling in lymphocytes. For example, insufficient (eg, low IgM levels) or misdirected humoral responses appear to be a common outcome of attenuated CARD11 signaling with or without increased IgE levels. A number of families presented with more severe humoral defects resembling CVID, which might reflect both intrinsic defects in B-cell differentiation and/or poor T-cell help. Future studies aimed at elucidating specific abnormalities in class-switch recombination and plasma cell differentiation in patients' B cells would be helpful. The neutropenia noted in several patients was not associated with obvious bone marrow defects, which could suggest an autoimmune cause; indeed, CARD11 is primarily expressed in mature lymphocytes. However, given that this is a diagnosis of exclusion, further investigation is warranted.
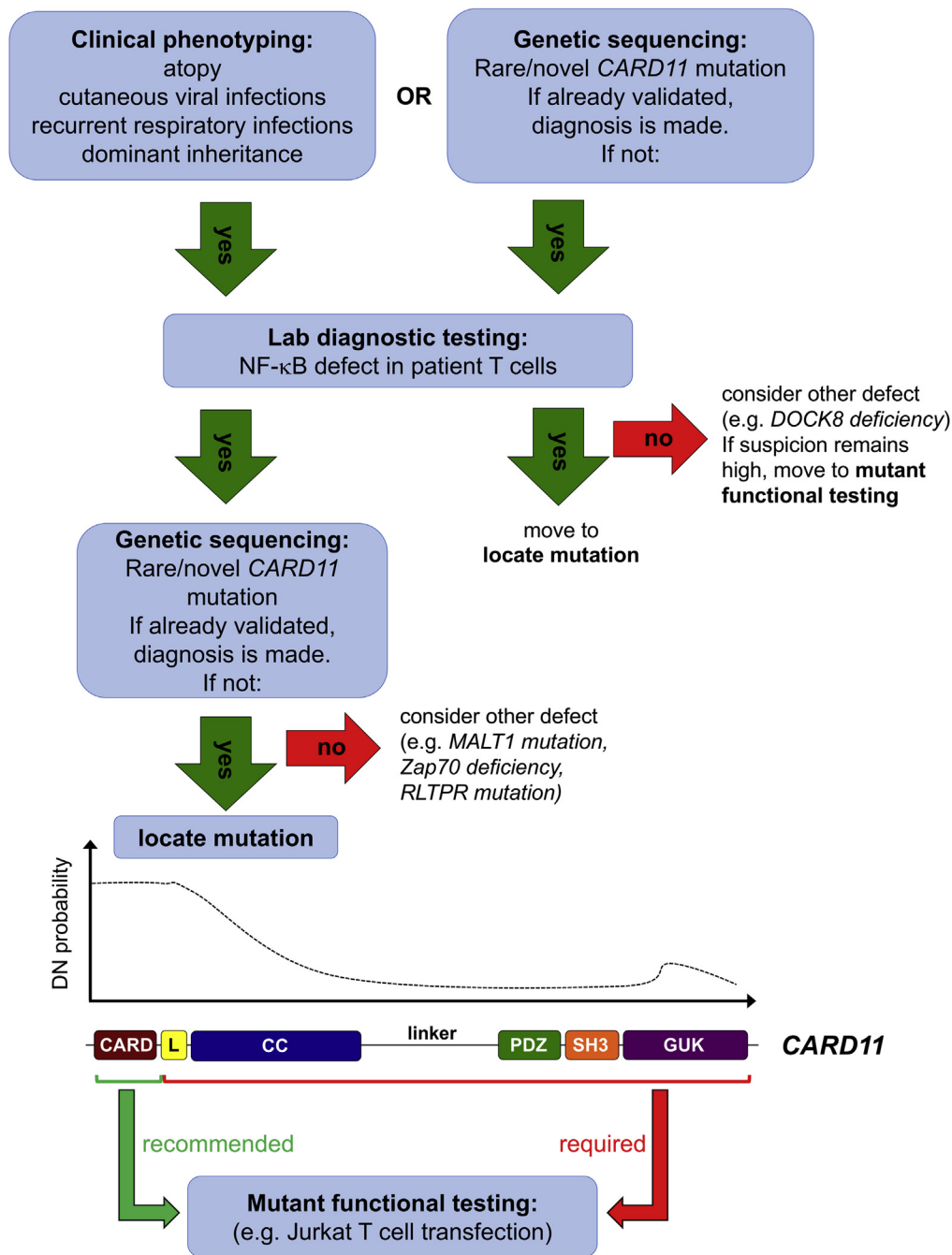
FIG 6. Clinical diagnostic algorithm for recognizing patients with *CARD11* DN mutations as a schematic diagram. Suspected patients typically present with atopy with or without cutaneous viral infections and respiratory tract infections. Simple laboratory diagnostic tests to pinpoint TCR-induced NF-κB activation defects in primary T cells from patients (eg, phospho-p65 and IκB degradation) are recommended before genomic sequencing analysis or after a *CARD11* mutation is uncovered (eg, through WES). Within these selected patients, a mutation in the CARD domain (or N-terminal CC domain) is highly likely to be DN, whereas mutations in the rest of the protein are more likely benign. Functional testing (eg, Jurkat transfection assays for NF-κB activation) is recommended for all novel CARD11 variants, especially for those outside the CARD domain.

Cutaneous viral infections (eg, molluscum and herpes simplex virus 1) were also common to several patients. Impaired CD8$^+$ T-cell immunosurveillance could be a factor and might also help to explain tumor development in certain patients. Interestingly, patients with BENTA carrying GOF *CARD11* mutations often present with molluscum and other viral infections (eg, EBV) and are at greater risk of lymphoma/leukemia development.[5] Unlike many patients with *CARD11* DN mutations, T cells from patients with BENTA are only mildly "anergic" and proliferate relatively well in response to robust stimuli, even though IL-2

production is often reduced.[6,34] There is also no evidence of T_H2 skewing or atopy in patients with BENTA described to date, although this has not been investigated thoroughly. Further studies are needed to elucidate how dysregulated CARD11 variant signaling leads to abnormal $CD4^+$ and $CD8^+$ T-cell responses that might predict expressivity of associated phenotypes (eg, atopy and viral skin infections). Based on our work and the work of others, we suspect alterations in TCR signal strength, metabolic reprogramming, and actin-dependent adhesion and motility could all be contributing factors.[13,35-38]

Our workup of 48 new patients encompassing 25 novel/rare variants further clarifies whether mutations in specific regions of CARD11 are more or less likely to be pathogenic (Fig 6). Notably, missense mutations in the N-terminal CARD domain (amino acids 1-110) are most likely to disrupt NF-κB (and, less reliably, mTORC1) signaling, probably by compromising interactions with BCL10 (and, by association, MALT1). The N-terminal CC domain (amino acids 130-200) is also a hotspot for pathogenic mutations, although it is still difficult to predict which variants in the CC domain will be LOF or DN; GOF mutations have been identified in the CARD, LATCH, and CC domains.[28,39] In contrast, we have not found DN mutations residing between residues approximately 200 to 970, encompassing the C-terminal portion of the CC domain, the flexible linker, and the PDZ and SH3 domains. In fact, 2 mutations within this region (p.P495S and p.R848C) significantly boosted TCR-induced NF-κB activity in Jurkat cells; however, more work is required to determine whether and how this effect contributes to autoimmune manifestations in these patients. Unlike CARD/CC-associated GOF mutations found in patients with BENTA, these mutations did not drive constitutive NF-κB activation in the absence of antigen receptor stimulation. The linker itself (amino acids 449-667) contains an array of redundant repressive and activating elements that govern the complex intramolecular regulation of CARD11,[40,41] making it unlikely to find single point mutations in the linker that affect CARD11 signaling. Finally, one new (p.R974C) and one previously confirmed DN mutation (p.R975W) were located in the guanylate kinase (GUK) domain, although nearby variants in this region showed no effect on TCR-induced NF-kB (p.V983M, p.E1028K, and p.D1152N).

In the end, LOF and/or DN activity was not detected in all rare variants from patients referred for a variety of phenotypes, including severe atopy. These results highlight the utility of our simple cell transfection assay in addition to the workup of primary patient cells whenever possible; indeed, as highlighted by the patient with the p.V195L mutation, the observed NF-κB signaling defect detected in primary cells cannot always be ascribed to DN activity. Although defects in mTORC1 signaling are also important, even small perturbations in cell culture conditions make quantification of differences in S6 phosphorylation extremely challenging for both Jurkat and primary T cells. Therefore we cannot currently recommend phospho-S6 quantification after short-term stimulation as a diagnostic assay for CARD11 DN mutations. Our comprehensive allelic series suggests that for CARD11, protein domain architecture might predict functional consequences of specific mutations. However, this too will require broader and more detailed structure-function analyses of the CARD11 protein before predictions could be used for clinical diagnoses.

For clinicians, this study also provides an improved differential diagnosis for immune deficiency and dysregulation linked to CARD11 mutations. An algorithm detailing our strategy for identifying and diagnosing these patients is depicted in Fig 6. Therefore heterozygous CARD11 DN mutations might be suspected and sought, either through analysis of existing exomes or included in other gene sequencing panels, in patients with histories of atopy (especially AD), often in combination with sinopulmonary bacterial infections or cutaneous viral infections (Fig 6), especially when a dominant family history of any of those phenotypes is present. Failure to thrive, neutropenia, autoimmunity (eg, alopecia), specific antibody deficiency and/or CVID, and even lymphoma can also be noted. Even in patients without atopy but with a family history of dominant inheritance of any of the other phenotypes above, it might be worth testing for a heterozygous CARD11 DN mutation. A simple laboratory diagnostic test aimed at uncovering a TCR-induced NF-κB signaling defect in primary T cells is strongly recommended, even before sequencing is performed. Although identification of such mutations might not alter patient care currently, continued evaluation and reporting of new CARD11 variants (perhaps through a registry) will advance our understanding of specific phenotypic associations and hopefully inform future clinical management. Certainly, those with any such phenotypes in whom a rare heterozygous CARD11 mutation is found even by chance should lead to strong suspicion that it is causal, especially if it resides in the CARD domain. Nevertheless, functional tests, such as those described here, are imperative for definitive diagnosis.

Key messages

- *CARD11* **DN mutations are associated with a broader spectrum of human disease phenotypes than previously appreciated, extending beyond atopy to include cutaneous viral and respiratory tract infections, hypogammaglobulinemia, autoimmunity, neutropenia, and lymphoma.**

- **Pathogenic DN mutations are most likely located in the N-terminal CARD and CC domains of CARD11, compromising TCR-induced NF-κB activation.**

- **Clinicians should test for causative** *CARD11* **DN mutations in patients who present with an autosomal dominant pattern of atopy, viral skin infections, and/or respiratory tract infections and exhibit defective TCR-induced NF-κB activation** *in vitro*, **with or without impaired TCR-induced S6 phosphorylation.**

REFERENCES

1. Notarangelo LD, Kim MS, Walter JE, Lee YN. Human RAG mutations: biochemistry and clinical implications. Nat Rev Immunol 2016;16:234-46.

2. Juilland M, Thome M. Role of the CARMA1/BCL10/MALT1 complex in lymphoid malignancies. Curr Opin Hematol 2016;23:402-9.

3. Meininger I, Krappmann D. Lymphocyte signaling and activation by the CARMA1-BCL10-MALT1 signalosome. Biol Chem 2016;397:1315-33.

4. Turvey SE, Durandy A, Fischer A, Fung SY, Geha RS, Gewies A, et al. The CARD11-BCL10-MALT1 (CBM) signalosome complex: stepping into the limelight of human primary immunodeficiency. J Allergy Clin Immunol 2014;134:276-84.

5. Arjunaraja S, Angelus P, Su HC, Snow AL. Impaired control of Epstein–Barr virus infection in B-Cell expansion with NF-κB and T-cell anergy disease. Front Immunol 2018;9:198.

6. Snow AL, Xiao W, Stinson JR, Lu W, Chaigne-Delalande B, Zheng L, et al. Congenital B cell lymphocytosis explained by novel germline CARD11 mutations. J Exp Med 2012;209:2247-61.

7. Dadi H, Jones TA, Merico D, Sharfe N, Ovadia A, Schejter Y, et al. Combined immunodeficiency and atopy caused by a dominant negative mutation in caspase activation and recruitment domain family member 11 (CARD11). J Allergy Clin Immunol 2018;141:1818-30.e2.

8. Jun JE, Wilson LE, Vinuesa CG, Lesage S, Blery M, Miosge LA, et al. Identifying the MAGUK protein Carma-1 as a central regulator of humoral immune responses and atopy by genome-wide mouse mutagenesis. Immunity 2003;18:751-62.

9. Ma CA, Stinson JR, Zhang Y, Abbott JK, Weinreich MA, Hauk PJ, et al. Germline hypomorphic CARD11 mutations in severe atopic disease. Nat Genet 2017;49:1192-201.

10. Hara H, Yokosuka T, Hirakawa H, Ishihara C, Yasukawa S, Yamazaki M, et al. Clustering of CARMA1 through SH3-GUK domain interactions is required for its activation of NF-kappaB signalling. Nat Commun 2015;6:5555.

11. Tanner MJ, Hanel W, Gaffen SL, Lin X. CARMA1 coiled-coil domain is involved in the oligomerization and subcellular localization of CARMA1 and is required for T cell receptor-induced NF-kappaB activation. J Biol Chem 2007;282:17141-7.

12. Meyts I, Bosch B, Bolze A, Boisson B, Itan Y, Belkadi A, et al. Exome and genome sequencing for inborn errors of immunity. J Allergy Clin Immunol 2016;138:957-69.

13. Lyons JJ, Milner JD. Primary atopic disorders. J Exp Med 2018;215:1009-22.

14. Adzhubei I, Jordan DM, Sunyaev SR. Predicting functional effect of human missense mutations using PolyPhen-2. Curr Protoc Hum Genet 2013Chapter 7: Unit 7.20.

15. Kircher M, Witten DM, Jain P, O'Roak BJ, Cooper GM, Shendure J. A general framework for estimating the relative pathogenicity of human genetic variants. Nat Genet 2014;46:310-5.

16. Kumar P, Henikoff S, Ng PC. Predicting the effects of coding non-synonymous variants on protein function using the SIFT algorithm. Nat Protoc 2009;4:1073-81.

17. Schubert D, Klein MC, Hassdenteufel S, Caballero-Oteyza A, Yang L, Proietti M, et al. Plasma cell deficiency in human subjects with heterozygous mutations in Sec61 translocon alpha 1 subunit (SEC61A1). J Allergy Clin Immunol 2018;141:1427-38.

18. Silberstein M, Tzemach A, Dovgolevsky N, Fishelson M, Schuster A, Geiger D. Online system for faster multipoint linkage analysis via parallel execution on thousands of personal computers. Am J Hum Genet 2006;78:922-35.

19. Silberstein M, Weissbrod O, Otten L, Tzemach A, Anisenia A, Shtark O, et al. A system for exact and approximate genetic linkage analysis of SNP data in large pedigrees. Bioinformatics 2013;29:197-205.

20. Gower JC. A general coefficient of similarity and some of its properties. Biometrics 1971;857-71.

21. Kaufman L, Rousseeuw PJ. Finding Groups in Data: An Introduction to Cluster Analysis. Hoboken (NJ): John Wiley & Sons; 2009.

22. Maechler M, Rousseeuw P, Struyf A, Hubert M, Hornik K. Cluster: cluster analysis basics and extensions. R package version. 2012;1:56.

23. Van Der Maaten L. Accelerating t-SNE using tree-based algorithms. J Machine Learning Res 2014;15:3221-45.

24. Witten IH, Frank E, Hall MA, Pal CJ. Data Mining: Practical Machine Learning Tools and Techniques. Burlington (MA): Morgan Kaufmann; 2016.

25. Yu L, Liu H, editors. Feature selection for high-dimensional data: a fast correlation-based filter solution. In: Proceedings of the 20th International Conference on Machine Learning (ICML-03); 2003. pp. 856-63.

26. Landwehr N, Hall M, Frank E. Logistic model trees. Machine Learning 2005;59:161-205.

27. Fuchs S, Rensing-Ehl A, Pannicke U, Lorenz MR, Fisch P, Jeelall Y, et al. Omenn syndrome associated with a functional reversion due to a somatic second-site mutation in CARD11 deficiency. Blood 2015;126:1658-69.

28. Chan W, Schaffer TB, Pomerantz JL. A quantitative signaling screen identifies CARD11 mutations in the CARD and LATCH domains that induce Bcl10 ubiquitination and human lymphoma cell survival. Mol Cell Biol 2013;33:429-43.

29. Thome M, Charton JE, Pelzer C, Hailfinger S. Antigen receptor signaling to NF-kappaB via CARMA1, BCL10, and MALT1. Cold Spring Harb Perspect Biol 2010;2:a003004.

30. Hamilton KS, Phong B, Corey C, Cheng J, Gorentla B, Zhong X, et al. T cell receptor-dependent activation of mTOR signaling in T cells is mediated by Carma1 and MALT1, but not Bcl10. Sci Signal 2014;7:ra55.

31. Shi JH, Sun SC. TCR signaling to NF-kappaB and mTORC1: expanding roles of the CARMA1 complex. Mol Immunol 2015;68:546-57.

32. Greil J, Rausch T, Giese T, Bandapalli OR, Daniel V, Bekeredjian-Ding I, et al. Whole-exome sequencing links caspase recruitment domain 11 (CARD11) inactivation to severe combined immunodeficiency. J Allergy Clin Immunol 2013;131:1376-83.e3.

33. Stepensky P, Keller B, Buchta M, Kienzler AK, Elpeleg O, Somech R, et al. Deficiency of caspase recruitment domain family, member 11 (CARD11), causes profound combined immunodeficiency in human subjects. J Allergy Clin Immunol 2013;131:477-85.e1.

34. Brohl AS, Stinson JR, Su HC, Badgett T, Jennings CD, Sukumar G, et al. Germline CARD11 mutation in a patient with severe congenital B cell lymphocytosis. J Clin Immunol 2015;35:32-46.

35. Aronica MA, Mora AL, Mitchell DB, Finn PW, Johnson JE, Sheller JR, et al. Preferential role for NF-kappa B/Rel signaling in the type 1 but not type 2 T cell-dependent immune response in vivo. J Immunol 1999;163:5116-24.

36. Pollizzi KN, Powell JD. Integrating canonical and metabolic signalling programmes in the regulation of T cell responses. Nat Rev Immunol 2014;14:435-46.

37. Rebeaud F, Hailfinger S, Posevitz-Fejfar A, Tapernoux M, Moser R, Rueda D, et al. The proteolytic activity of the paracaspase MALT1 is key in T cell activation. Nat Immunol 2008;9:272-81.

38. Rueda D, Gaide O, Ho L, Lewkowicz E, Niedergang F, Hailfinger S, et al. Bcl10 controls TCR- and FcgammaR-induced actin polymerization. J Immunol 2007;178:4373-84.

39. Lenz G, Davis RE, Ngo VN, Lam L, George TC, Wright GW, et al. Oncogenic CARD11 mutations in human diffuse large B cell lymphoma. Science 2008;319:1676-9.

40. Jattani RP, Tritapoe JM, Pomerantz JL. Cooperative control of caspase recruitment domain-containing protein 11 (CARD11) signaling by an unusual array of redundant repressive elements. J Biol Chem 2016;291:8324-36.

41. Jattani RP, Tritapoe JM, Pomerantz JL. Intramolecular interactions and regulation of cofactor binding by the four repressive elements in the caspase recruitment domain-containing protein 11 (CARD11) inhibitory domain. J Biol Chem 2016;291:8338-48.